Surface Science
## Room 120 - Session SS+2D+AMS-WeA

Defects Nanoarchitecture and Complex Systems
Moderators: Dario Stacchiola, Brookhaven National Laboratory, **Zhenrong Zhang**, Baylor University

2:30pm SS+2D+AMS-WeA-2 Molecular Sensing ZnO Surfaces Studied by Operando Low-Energy Ion Beam Analysis, *Taku Suzuki, Y. Adachi, T. Ogaki, I. Sakaguchi,* National Institute for Materials Science, Japan

1. Introduction

The basic mechanism of the resistive gas sensing has been established; it is essentially a redox reaction of the surface mediated by the negatively charged oxygen adsorbate. For example, the sensing of ethanol (EtOH) with the ionosorbed oxygen of O^{2-} is written as,

$$EtOH(ads) + O^{2-}(ads) \rightarrow CH_3CHO + H_2O + 2e-, (1)$$
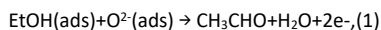
where (ads) denotes an adsorbate. It is reasonable to assume that the gas sensing properties differ between crystallographic atomic planes. Indeed, the crystal plane dependent gas sensing response has been studied by many research groups in the last decade for EtOH sensing by ZnO, which is one of the most intensively studied target gas – sensing material combinations. The specific knowledge of the crystal plane dependence of gas sensing is useful for the development of sensing materials.

The ZnO crystal plane dependence of the gas sensing properties has typically been studied using a nanocrystal. However, the effect resulting from the contact between the particles has hindered straightforward interpretation. To overcome this problem, the ZnO crystal plane dependence of the EtOH sensing was investigated using an analytical approach in the present study, namely low-energy ion scattering spectroscopy (LEIS) combined with the pulsed jet technique.

2. Method: LEIS combined with pulsed jet

We applied a newly developed He+ LEIS combined with the pulsed jet technique to analyze the surface structure of ZnO during the EtOH sensing. In this novel technique, the free gas jet is periodically blown onto the sample surface to simulate the gas sensing surface in a vacuum as one under the realistic working condition, while the background pressure is kept low enough for the operation of He+ LEIS.

The sample was ZnO single crystals with an atomically flat mirror-polished surface. Four dominant low-index surfaces, which are Zn-terminated (0001) (*c*(+)), O-terminated (0001) (*c*(-)), (10-10) (*m*), and (11-20) (*a*), were used to evaluate the crystal orientation dependent gas sensing properties.

References

[1] N. Saito et al., Chemical Sensors 39(2023)108. (Japanese)

[2] T. Suzuki et al., Surfaces and Interfaces 35(2022)102371.

[3] T. Suzuki et al., Appl.Surf.Sci.538(2021)148102.

2:45pm SS+2D+AMS-WeA-3 Finding Surface Defects in Electronic Materials, *Sujitra Pookpanratana,* National Institute of Standards and Technology **INVITED**

All electronic materials contain a wide range of defects ranging in length scales from point defects to micrometer (or sub-millimeter) scale features. Some defects can be beneficial, benign, or detrimental to the functionality of the material. It's critical to identify and locate defects, and determine their impact in the host material. Here, I will highlight the identification of defects and their impact in 2D graphene�based systems and wide bandgap semiconductors using photoemission electron microscopy (PEEM). PEEM is a nanoscale, surface-sensitive, full-field imaging technique based on the photoelectric effect. PEEM provides real space imaging of surfaces with enhanced contrast mechanism based on topographic and electronic properties, and measurement of electronic properties. In the first example, we image epitaxial graphene (EG) topography in real space and measure the electronic structure of monolayer EG regions with micrometer-scale angle resolved photoemission (μ-ARPES). We detect characteristic electronic features of graphene such as the Dirac points and the π-band, and the electronic flat band at region with different contrast [1]. Through Raman spectroscopy on the same regions that were analyzed by PEEM, and we estimated a significant amount of compressive strain (~1.2%) coinciding with the flat band region [1]. In the second example, we highlight the full-field PEEM capability by following the de�and re-intercalation of 2D Ag within EG under heating conditions. For the 2D Ag system, we find Ag clusters initially diffuse to the top EG surface and finally re-intercalate through defects with the Ag intercalation front to be 0.5 nm s-1 ± 0.2 nm s-1 [2]. The EG defects serve as intercalation "doors." Lastly, we will show extended surface defects propagating through epitaxy GaN and β-Ga2O3 which also induce the presence of bandgap states.

[1] F. Niefind, H. G. Bell, T. Mai, A. W. Hight Walker, R. E. Elmquist, S. Pookpanratana, J. Appl. Phys. 131, 015303 (2022).

[2] F. Niefind, Q. Mao, N. Nayir, M. Kowalik, J. J. Ahn, A. Winchester, C. Dong, R. A. Maniyara, J. Robinson, A. van Duin, and S. Pookpanratana, Small 20, 2306554 (2024).

3:15pm SS+2D+AMS-WeA-5 SSD Morton S. Traum Award Finalist Talk: Silver Iodide – Surface Structure and Ice Nucleation Investigated by Noncontact AFM, *Johanna Hütner[1], D. Kugler,* Vienna University of Technology, Austria*; F. Sabath,* Bielefeld University, Germany*; M. Schmid,* Vienna University of Technology, Austria*; A. Kühnle,* Bielefeld University, Germany*; U. Diebold, J. Balajka,* Vienna University of Technology, Austria

Silver iodide (AgI) is used as a cloud seeding material due to its ability to nucleate ice efficiently, which is explained by the good lattice match between AgI and hexagonal ice. The basal (0001) cleavage plane of AgI deviates from the lattice of hexagonal ice by as little as 2.5%. However, AgI consists of stacked planes of positively charged Ag^+ alternating with negatively charged I^-. Cleaving a AgI crystal along the (0001) plane thus exposes Ag^+ and I^- terminated surfaces. Both terminations are polar and inherently unstable.

We present atomically resolved noncontact atomic force microscopy (NC-AFM) images that show how AgI(0001) surfaces compensate for this non-zero electric dipole perpendicular to the surface. Both Ag and I terminated surfaces form reconstructions, whose structure affects their ice nucleating abilities. NC-AFM images of UHV cleaved surfaces exposed to water vapor reveal that ice forms an epitaxial layer only on the Ag terminated surface, whereas on the I termination ice forms three-dimensional clusters.

These atomic-level observations could enhance our understanding of ice formation processes in the atmosphere.

3:30pm SS+2D+AMS-WeA-6 SSD Morton S. Traum Award Finalist Talk: Reversible Non-Metal to Metal Transition and Effective Debye Temperatures of Highly Crystalline NiFe₂O₄ Thin Films, *Arjun Subedi[2], D. Yang, X. Xu, P. Dowben,* University of Nebraska-Lincoln, USA

The surface of $NiFe_2O_4$ thin film undergoes a conductivity change with temperature. X-ray photoelectron spectroscopy (XPS) of $NiFe_2O_4$ thin film at room temperature showed large binding energy shifts in Ni $2p_{3/2}$, Fe $2p_{3/2}$, and O 1s core levels, due to photovoltaic surface charging indicating that prepared $NiFe_2O_4$ thin film was dielectric or non-metallic at room temperature. The core level binding energy shifts, due to photovoltaic surface charging, were found to be around 5 eV for each of the core levels at room temperature. The core level binding energy shifts decreased when the thin film was annealed in vacuum. The XPS core level binding energy shifts from the expected values became negligible at an elevated temperature of 410 K and beyond. This suggests that $NiFe_2O_4$ thin film became metallic at the temperature of 410 K and beyond. When the sample cooled down to room temperature, the sample reversibly became more dielectric, showing again the same core level binding energy shifts of 5 eV. Such reversible phase change of the thin film was further supported by the reversible Fermi edge shift with temperature. Low energy electron diffraction (LEED) images, taken for the $NiFe_2O_4$ thin film surface, showed that the surface was highly crystalline throughout the reversible temperature controlled non-metal to metal transition. The XPS spectra of Ni $2p_{3/2}$, Fe $2p_{3/2}$, and O 1s core levels taken at different temperatures showed that the changes in core level binding energies followed a proposed Arrhenius-type model with temperature. The effective bulk Debye temperatures of 629.10 ± 58.22 K and 787.03 ± 52.81 K were estimated using temperature dependent intensities of Fe $2p_{3/2}$ and Ni $2p_{3/2}$ XPS spectra respectively indicative of different sites for Fe and Ni. The effective surface Debye temperature of 249.7 ± 11.1 K was estimated using temperature dependent intensities of LEED. Lower effective Debye temperature was observed for surface, as expected. The phase transition, the estimates of the effective Debye temperatures, and the model applied to the core level binding changes with temperature altogether shed light on the fundamental properties of the material with temperature.

---

[1] **SSD Morton S. Traum Award Finalist**
[2] **SSD Morton S. Traum Award Finalist**

4:15pm SS+2D+AMS-WeA-9 In situ Structure Study of a MnOX-Na2WO4/SiO2 Catalyst for OCM under Na₂WO₄ Melting Conditions, *Yong Yang,* ShanhaiTech University, China; *D. Wang, E. Vovk,* Shanghaitech.edu.cn, China; *Y. Liu, J. Lang,* ShanghaiTech University, China

MnO_x-Na_2WO_4/SiO_2 catalyst exhibited notable C_2 selectivity/yield in the oxidative coupling of methane (OCM), a promised green chemistry reaction[1, 2]. Nevertheless, the reaction mechanism of this catalyst remains a subject of contention, particularly regarding the role of Na_2WO_4 in the activation[3, 4]. In this study, *in situ* characterizations of a TiO_2-modified MnO_x-Na_2WO_4/SiO_2 catalyst, are conducted by XRD and XPS correlating to the OCM reaction condition, focusing on the simultaneous phase transition of catalyst components within its activation temperature zone. The online MS along with XPS/XRD coupled activity study confirm that transition from Mn^{3+} to Mn^{2+} stands as a pivotal factor influencing the reactivity. *In situ* XRD further revealed that in this narrow temperature window there is a particular three-step Na_2WO_4 phase change, ending as molten salt, right before the substantial Mn^{3+} to Mn^{2+} transfer initiated. In addition, the rarely observed Na_2WO_4 behavior as molten salt is obtained by *in situ* XPS with rapid spectra collected during an on-stage heating process. A sensitive self-reduction of the tungsten upon heating to melting point is found. These comprehensive *in situ* catalyst characterizations, covering the extensive structure-activity relationship from solid state to partial molten salt condition, providing a interlocking pathway for the reactive oxygen species transfering at high temperature. The results provides new important insight into the complex MnO_x-Na_2WO_4/SiO_2 catalyst as a key to understand the activation mechanism of NaWMnSi catalyst in OCM.

[1] Lunsford JH, Catalytic conversion of methane to more useful chemicals and fuels: a challenge for the 21st century. Catalysis today 63 (2000) 165-174;

[2] Lunsford JH The Catalytic Oxidative Coupling of Methane. Angewandte Chemie International Edition in English 34 (1995) 970-980;

[3] Si J, Zhao G, Sun W, Liu J, Guan C, Yang Y, Shi XR, Lu Y Oxidative Coupling of Methane: Examining the Inactivity of the MnOx-Na2WO4/SiO2 Catalyst at Low Temperature. Angewandte Chemie International Edition 61 (2022) e202117201

[4] Fang X, Li S, Gu J, Yang D Preparation and characterization of W-Mn catalyst for oxidative coupling of methane. J Mol Catal 6 (1992) 255-261

4:30pm SS+2D+AMS-WeA-10 Characterization of Nanoplastics Samples, *T. Roorda, M. Brohet, S. Campos Jara,* **Irene Groot**, Leiden University, Netherlands

Plastic particles in the ocean have become a contaminant of emerging concern due to their damage to humans and marine animals. Of all plastic production, which is increasing still, it has been shown that more than 99% of plastic waste which ends up in the oceans cannot be accounted for. The belief is that all of this plastic degrades to a nano-sized scale which is extremely hard to detect. In order to understand the fate of nanoplastics in aquatic environments, we must have a better understanding of the degradation mechanisms at an atomic and chemical level. In this project, we have developed procedures to evaporate powdered materials and deposit them onto a prepared surface. The deposition of nanoplastics is confirmed by mass spectrometry, Auger electron spectroscopy, and X-ray photoelectron spectroscopy. Using atomic force microscopy combined with scanning tunneling microscopy, the deposited plastics are investigated.

We also investigate plastics samples after several degradation mechanisms, such as oxygenation, hydrogenation, UV exposure, and thermal annealing. After degradation, the plastics samples are studied in ultra-high vacuum with atomic force microscopy combined with scanning tunneling microscopy and with X-ray photoelectron spectroscopy.

4:45pm SS+2D+AMS-WeA-11 Oxidation of NiCr and NiCrMo- Unraveling the Role of Mo with XPEEM Studies, *Keithen Orson, D. Jessup,* University of Virginia; *W. Blades,* Juniata College; *J. Sadowski,* Brookhaven National Laboratory; *Y. Niu, A. Zakharov,* Lund University, Sweden; *P. Reinke,* University of Virginia

Nickel-chromium based superalloys combine good mechanical strength with excellent resistance to corrosion over a wide range of conditions. Passivity stems primarily from a thin layer of chromium oxides and hydroxides and increasing Cr content above a threshold of 11-15wt% results in a protective passive layer. Adding minor alloying elements like Mo has an outsized impact on corrosion resistance, but there is debate in literature over the mechanism of this action. To investigate the interplay of Cr concentration and Mo alloying, the early-stage oxidation (0-65 Langmuir of O_2) of Ni22Cr, Ni5Cr, and Ni22Cr6Mo were studied on a clean metal surface and moderate temperatures (450-500˚C). The oxidization was studied in-situ using x-ray photoelectron microscopy (XPEEM), which yields x-ray absorption hyperspectral images at 0, 5, 20, and 65 L of exposure, and a timeseries observing the oxide evolution from 0 to 65L at a single photon energy representative of Cr_2O_3. XPEEM valence band spectra, and conventional XPS study of the same samples complement the experiment. To analyze the ~10^7 spectra produced by hyperspectral imaging, several data dimensionality reduction techniques including principal component analysis and non-negative matrix analysis were used to gain insight into the oxide evolution, the species present, and their spatial distribution. The amounts of each species present in the hyperspectral images were quantified using cosine similarity. Oxidation of Ni22Cr produces islands of Cr_2O_3 along with a surface oxide, while on Ni5Cr larger, sparser islands are observed. For both binary alloys the oxide grows in a layer-plus-island morphology. The oxide island chemistry of Ni5Cr appears to include some NiO as well as Cr_2O_3. Ni22Cr6Mo, on the other hand, does not nucleate oxide islands visible with XPEEM but instead forms a continuous oxide layer whose thickness increases over time. This is commensurate with a layer-by-layer growth mode which is a significant advantage for protective function. This observation has implications for Mo's protective mechanism in the passive film, suggesting that Mo may be protecting from localized breakdown by altering the morphology of the oxide to produce a more uniformly protective oxide layer.

5:00pm SS+2D+AMS-WeA-12 An Investigation of Local Distortions on High Entropy Alloy Surfaces, *Lauren Kim,* University of Wyoming; *P. Sharma,* Lehigh University; *G. Balasubramanian,* lehigh University; *T. Chien,* University of Wyoming

High entropy alloys (HEAs) are a widely studied family of materials that typically contain five or more elements. There are many combinations of elements that can create HEAs, and material properties can be tuned simply by changing elemental compositions. These properties of HEAs result in numerous applications, such as catalysis, energy storage, and aerospace engineering refractory materials. Severe-lattice-distortion is identified as one of the four core effects impacting the physical properties in HEAs. In this work, we demonstrate atomic resolution images of the surface of a CrMnFeCoNi HEA (Cantor alloy) using scanning tunneling microscopy (STM). This data allows us to determine lattice local distortions unambiguously. Additionally, we report our findings on the types of local defects on the surface, such as grain boundaries, phase changes, and amorphization, and how these defects can impact local distortions of the crystals nearby.

5:15pm SS+2D+AMS-WeA-13 Grain Boundary and Twin Boundary Solute Segregations in Nanocrystalline Al-Mg Alloy, *Xuanyu Sheng, z. Shang, A. Shang,* Purdue University, China; *H. Wang, X. Zhang,* Purdue University

Chemical segregations at grain boundaries (GBs) have been broadly investigated in Al alloys. However, there are limited experimental evidence demonstrating the dependence of solute segregation on GB characteristics. Here, we quantified solute segregation at GBs in nanocrystalline Al-1Mg (at.%) alloy by combining energy-dispersive X-ray spectroscopy, high-resolution scanning transmission electron microscopy and automated crystallographic indexing and orientation mapping. The dependence of solute segregation on the grain boundary misorientation angle is analyzed. Due to their higher excess free volume, high angle grain boundaries contain more Mg solutes than the low angle grain boundaries. Furthermore, coherent twin boundaries (CTBs) exhibit low solute segregation. However, incoherent twin boundaries (ITBs) display greater solute concentration. The different solute segregation behavior between CTBs and ITBs originates from their grain boundary structure. The solute segregation behavior reported here may shed light on the GB engineering of Al alloys.

5:30pm SS+2D+AMS-WeA-14 Charge Ordering Phase Transition in Bilayer Sn on Si(111), *Nathan Guisinger, M. Chan,* Argonne National Laboratory; *C. Lilley,* University of Illinois - Chicago

The atomic-scale investigation of the "bilayer" reconstruction of Sn on heavily doped n-type Si(111) was performed with scanning tunneling microscopy. When cooled to 55K, the bilayer reconstruction undergoes both a structural and electronic transition. Structurally, the dimer units of the bilayer shift to form a herringbone pattern with a rhombohedral ordering. The electronic structure transitions into a very uniform square lattice with similar dimensions to the structural dimers. There are distinct differences between the structural and electronic spacing that resolves itself when counting multiple periods. This ordering is like behavior observed in materials that exhibit charge density waves. Furthermore, STS point spectra show a transition from a small gap to a large insulating gap at

low temperature that is consistent with a transition to a Mott insulating ground state. The charge ordering coupled with the relaxation to a Mott insulating phase upon cooling the Sn bilayer presents unique physics when the dimensionality is reduced from the bulk.

5:45pm **SS+2D+AMS-WeA-15 SSD Morton S. Traum Award Finalist Talk: On-Surface Design of Highly-Ordered Two-Dimensional Networks Stabilized by Nonmetal Atoms**, *Alisson Ceccatto*[1], University of Campinas (UNICAMP), Brazil; *G. Campi,* Yachay Tech University, Ecuador; *V. Carreño, E. Ferreira,* University of Campinas (UNICAMP), Brazil; *N. Waleska-Wellnhofer, E. Freiberger, S. Jaekel,* Friedrich-Alexander-University Erlangen-Nürnberg (FAU), Germany; *C. Papp,* Freie Universität Berlin, Germany; *H. Steinrück,* Friedrich-Alexander-University Erlangen-Nürnberg (FAU), Germany; *D. Mowbray,* Yachay Tech University, Ecuador; *A. de Siervo,* University of Campinas (UNICAMP), Brazil

Supramolecular nanoarchitectures have been widely explored to precisely design low-dimensional materials at atomic and molecular levels [1]. Such control is mainly based on bottom-up fabrication methods, e.g. on-surface synthesis, by combining molecular building blocks and atoms to engineer novel nanomaterials [2]. Particularly, the self-assembled monolayers (SAMs) of organic molecules present the potential for applications in nanoelectronics due to their reversible non-covalent interactions [3]. Such intermolecular interactions allow the fabrication of almost defect-free supramolecular nanostructures. Typically, the geometry of these nanoarchitectures can be controlled by the insertion of metal and non-metal atoms in the reaction process. To date, the adatom-mediated SAM fabrication concentrates on the use of metal adatoms, especially d metals (Cu, Co, Au, and Fe) [4]. Herein, by combining scanning tunneling microscopy (STM) measurements and density functional theory (DFT) calculations, we report the 2D self-assembled of 1,3,5-tris[4-(pyridin-4-yl)-[1,1'-biphenyl])benzene (TPyPPB) molecules on Ag(111) in the presence of Cl adatoms. The adsorption of the TPyPPB molecules on the clean Ag(111) surface forms an almost defect-free porous SAM stabilized by hydrogen bonds, so-called triangular packing. Such packing can be explored as a host-guest material for atom/molecular confinement. However, in the presence of Cl adatoms, the molecular arrangement changes dramatically. The molecular assembly changes its geometry, forming a non-porous SAM stabilized by H···Cl···H bonds. Such halogen-mediated SAM presents the advantage that the adatom used to stabilize the nanostructure has less influence on the electronic density compared to the typical metal adatoms.

Keywords: On-surface synthesis, STM, Self-assembly monolayer, Nanoporous networks.

References

1. Fan, Q. et al. Accounts of Chemical Research 48, 2484–2494 (2015).

2. Pawlak, R. et al. Journal of the American Chemical Society 142, 12568–12573 (2020)

3. Casalini, S. et al. Chemical Society Reviews 46, 40–71 (2017)

4. Shi, Z. et al. Journal of the American Chemical Society 133, 6150–6153 (2011)

---

[1] **SSD Morton S. Traum Award Finalist**

Author Index

Bold page numbers indicate presenter